Tungalag et al., 2023. Mongolian Geoscientist 28 (56)
DOI: https://doi.org/10.5564/mgs.v28i56.2427

Mongolian Geoscientist

Original Article

The Paleozoic Granitic Rocks from the Telmen Complex in the Tarvagatai Block, Central Mongolia: Petrogenesis, U-Pb geochronology, and its tectonic implications

Naidansuren Tungalag[1*], Bayaraa Ganbat [1,2], Sukhbat Baasansuren[1], Gansukh Orgil[1], Davaadorj Enktsatsral[1], Myagmarsuren Batmunkh[1]

[1]*Department of Magmatism and Metallogeny, Institute of Geology, Mongolian Academy of Sciences, Ulaanbaatar 15160, Mongolia*
[2]*CAS Key Laboratory of Crust-Mantle Materials and Environments, University of Science and Technology of China, Hefei 230026, China*

**Corresponding author: tungalag@mas.ac.mn, ORCID: 0000-0001-7073-8383*

ARTICLE INFO

Article history:
Received 30 October, 2022
Revised 27 January, 2023
Accepted 07 March, 2023

ABSTRACT

The Tarvagatai Block is located in the northern part of Central Mongolia, which is a widespread occurrence and occupies roughly 60% of the whole exposure along the Khangai fault and the Tarvagatai uplift. Granitic magmatism was emplacement during the Middle Paleozoic, which is predominantly composed of granite-granodiorite and gabbro-diorite and rarely gabbro. This article represents petrographical, geochemical, and U-Pb zircon age data from the Telmen Complex of the Tarvagatai Block, Central Mongolia. The U-Pb dating of zircon yields a Late Silurian emplacement age (419±3 Ma) for the Telmen Complex. Geochemically, the Telmen Complex is an I-type intrusion of metaluminous nature with a SiO_2 content ranging from 53.06 to 72.25 wt.% and mainly of medium to high K calc-alkaline series. Telmen Complex granites show enrichments in light rare earth elements, depletion in heavy rare earth elements, with a ratio of 4.053, $(La/Yb)_N$=9.15, and weak positive or normal Eu anomalies. A spider diagram indicates that these rocks are enriched in Ba, K, Pb, and Sr and depleted in Nb, Ta, and Ti. The Early Paleozoic Telmen Complex granitics have trace element features, for example, Nb-Ta depletions, which indicate that these rock units were emplaced in a convergent-margin setting and typical of the lower continental crust. In addition, the geochemical data show that the volcanic arc tectonic setting and, moreover, the continental arc array setting display on the Nb/Yb versus TiO_2/Yb diagrams. Therefore, we suggest that they were probably positioned in an active continental setting and in a Silurian ~419 Ma.

Keywords: Magmatism, geochemistry, Ordovician-Silurian granitic rocks, geodynamic settings.

INTRODUCTION

Central Mongolia is located between the Siberian Plate in the north, the North China Plate in the south and the Pacific plate in the east. It is an important portion of the southwestern margin of the Central Asian Orogenic Belt (CAOB) and records the collision of microcontinental massifs and terranes (Sengör et al., 1993; Windley et al., 2007; Jahn et al., 2004).

The Central Asian Orogenic Belt is considered to have a complex tectonic history (Jahn et al., 2000a, b; Windley et al., 2007, Schulman and Paterson, 2011, Liu et al., 2016; Chen et al.,

© The Author(s). 2022 **Open access** This article is distributed under the terms of the Creative Commons Attribution 4.0 International License (https://creativecommons.org/licenses/by/4.0/), which permits unrestricted use, distribution, and reproduction in any medium, provided you give appropriate credit to the original author(s) and source, provide a link to the Creative Commons license, and indicate if changes were made.

2017). Terminal closure of the Paleo-Asian Ocean resulted in a collision between North China and Siberia (Sun et al., 2004; Guan et al., 2018).

The Tarvagatai Block is located in the northern part of Central Mongolia and is a distribution of multiple stages of magmatism. The Paleozoic Telmen Complex was formed in the Tarvagatai Block, which plays a significant role in the crustal history and collisional tectonics of the CAOB (Fig. 1).

The Tarvagatai Block is characterized by a heterogeneous structure, consisting of the Early Precambrian complex, later Riphean lithotectonic complexes, Late Paleoproterozoic gabbro- anorthosite, and Early to Late Paleozoic granitic complexes (Kozakov et al., 2011).

The occurrence of older fragments indicates the presence of a Precambrian basement in the area; they comprise biotite and hornblende gneiss with rare enclaves of amphibolite and granitic gneisses. The Riphean Complex comprises alternating hornblende crystalline schists and biotite gneisses with marble horizons. The upper age limit of the Riphean Complex is determined by subautochthonous granitics with an age of about 810 Ma (Kozakov et al., 2011).

Granitic rocks are widespread occurrence and occupy about 60% of the whole exposure of the block. The variety of Paleozoic magmatic rocks includes Mid-Late Cambrian, Early-Late Ordovician, Late Devonian, Late Carboniferous, and Permian granitics. The age obtained for the granitics varies from 1784 Ma to 268 Ma

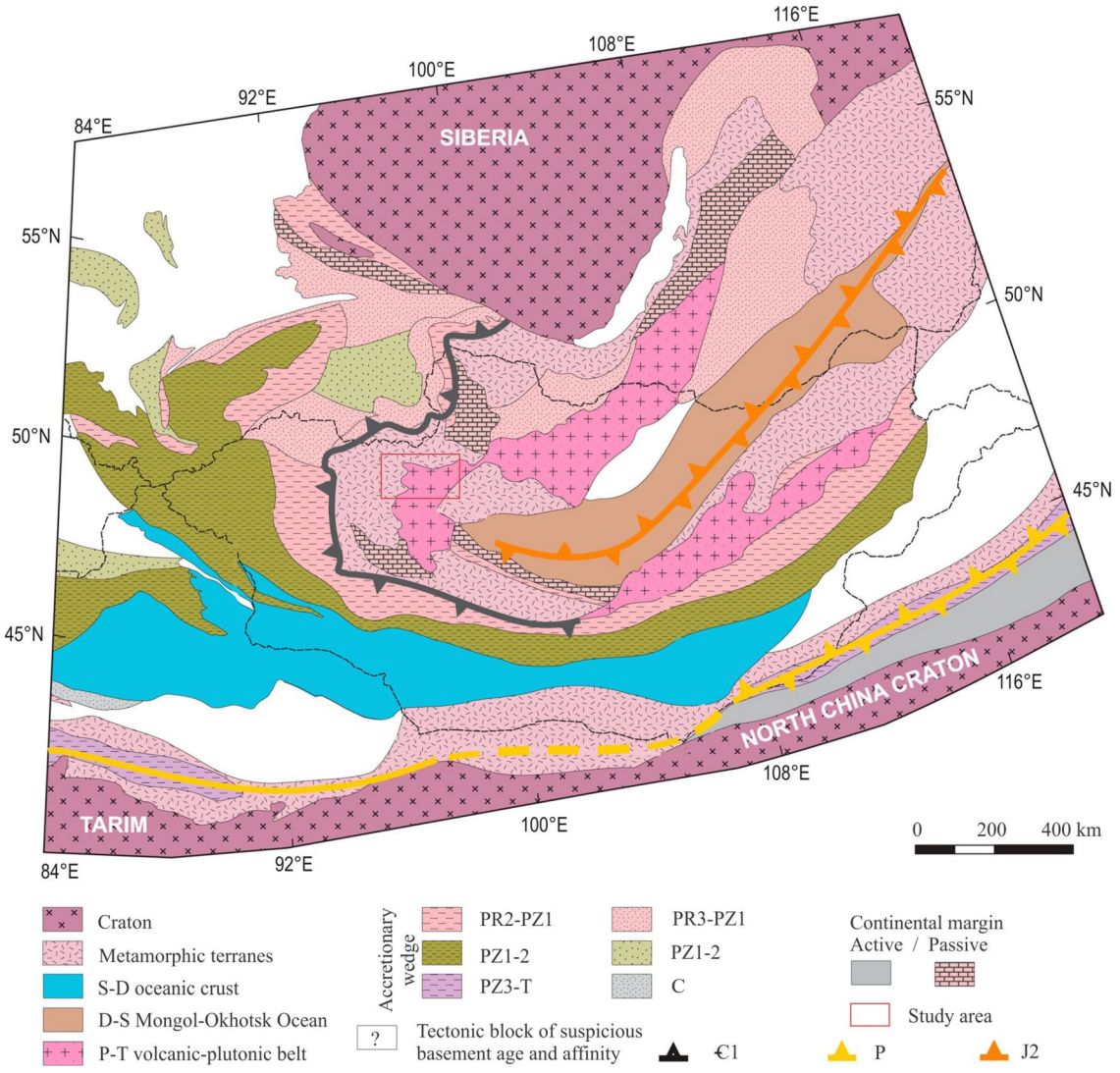

Fig. 1. Geological position of Mongolia in the CAOB framework, modified from (Hanžl et al., 2020)

(Anisimova et al., 2009; Kröner et al., 2014; Kozakov et al., 2011; Yarmolyuk et al., 2013, 2016, 2018, 2019), while (εNd(T) values of (Nd (T) vary from -3.2 to -5.8 and TNd (DM)=1.6-1.3 Ga) (hornblende diorite) (Kozakov et al., 2011; Yarmolyuk et al., 2016).

This article presents new whole-rock geochemical data, LA-ICP-MS zircon U-Pb dating, petrographic description, petrogenesis, and geodynamic setting of the Telmen Complex in the Tarvagatai Block.

GEOLOGICAL OUTLINE

Kheraskov (1966) originally identified the gabbro-plagogranite and gabbro-granodiorite rocks of the Mid-Late Cambrian Telmen Complex. These rocks are widely scattered in northern and Central Mongolia.

In recent years, through 1:200,000-scale mapping, granitic rocks of that age have been confirmed and distinguished in the Telmen Complex. Furthermore, some researchers compared the above-mentioned studies and analyzed them with granitics distinguished in Tuva, and it was distinguished as the Early-Late Ordovician Telmen Complex.

In our study area, the granitic rocks known as the Telmen Complex are distributed in the fault zone of the Ider River and its branches, which are highly affected by tectonics in the southwest and northeast trending zone. Almost 60% of the Telmen Complex in the Tarvagatai Block is occupied by the massive gabbro-diorite, quartz diorite, granodiorite of Phase I and monzodiorite, quartz monzonite, colored medium-grained biotite and biotite-amphibole granite of Phase II (Fig. 2).

Several detailed geochronological information is available for the Telmen Complex where the age of granodiorite is 446 Ma (Fedorov, 1966) and

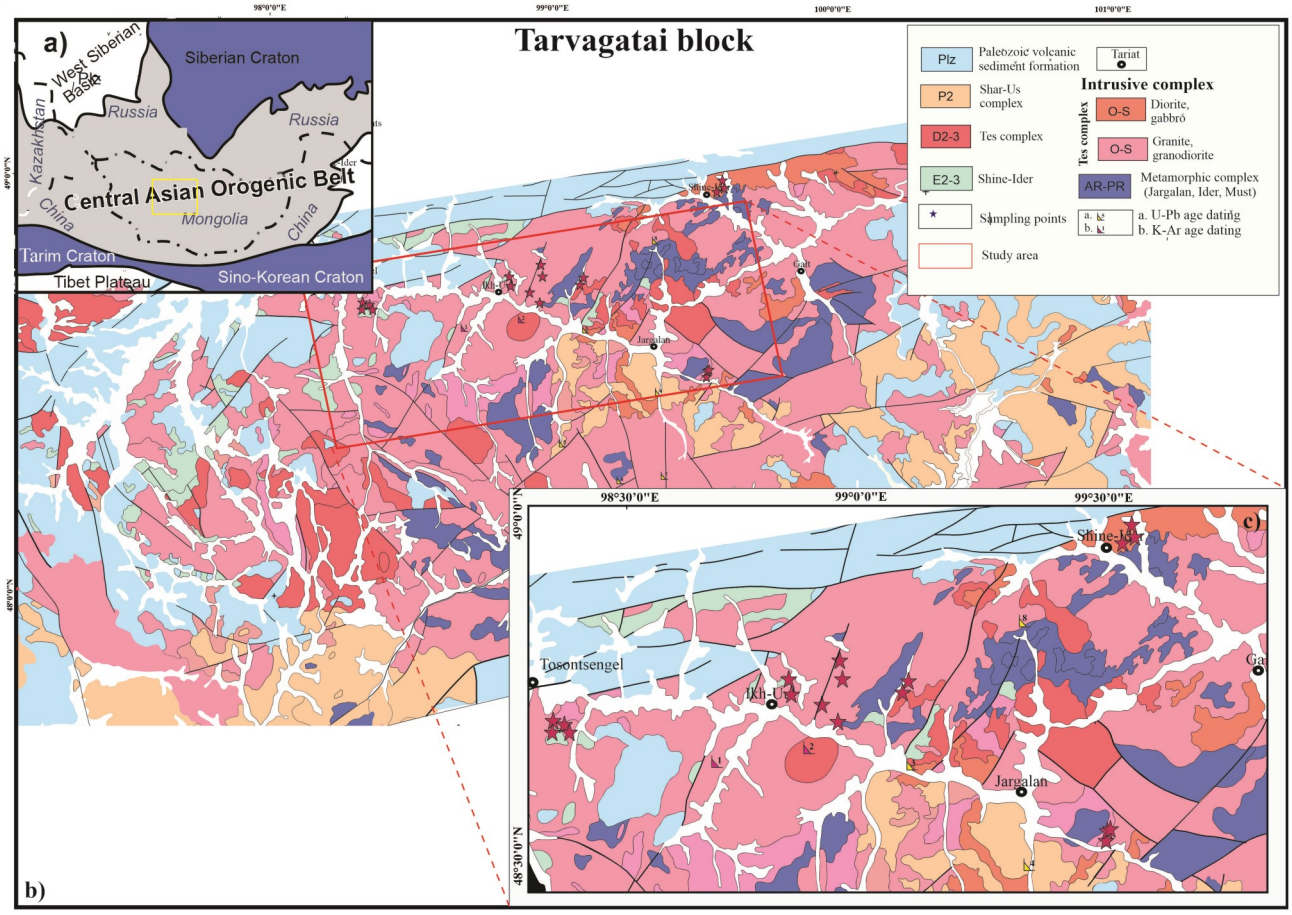

Fig. 2. a) Central Asian Orogenic Belt. b) Distribution map of granitics in the Tarvagatai Block, map scale 1:500 000 (modified after (Erdenechimeg et al., 2017), Geological ages: K-Ar age dating: (1) 446 Ma and (2) 226 Ma (Fedorov, 1966); U-Pb zircon dating: (3) 437±7 Ma (Kozakov et al., 2011), (4) 246±1 Ma, (5) 268±1 Ma and (7) 257±6 (Yarmolyuk et al., 2016), (6) 246±2 (Erdenechimeg et al., 2017), (8) 421±1 Ma (Kozakov et al., 2011)

the hornblende diorite is 437±7 Ma and 421±1 Ma (Kozakov et al., 2011) and the granodiorite is 419±3 Ma (this study), which may be represented by Late Ordovician to Silurian age.

SAMPLE DESCRIPTION AND PETROGRAPHY

The Telmen Complex forms a large rock outcrop outlook, the main units are characterized by a light gray appearance and comprise units whose mineral components can be identified directly by unaided eyes.

Nine samples from the Telmen Complex, and prepared into thin sections and examined on a polarizing microscope. Mineralogical features and textural variations observed in the hand specimens and outcrops are also reflected in their petrographic characteristics (Figs. 3a,b,c).

The medium-grained leucogranodiorite comprises plagioclase (35-40%), K-feldspar (20-25%), quartz (25-30%), biotite (8-10%), and minor amounts of zircon, apatite, and opaque constituents. Plagioclase occurs as large subhedral to anhedral crystals, polysynthetic twins, and the average size ranges between 0.3 and 2.8 mm (Fig. 4a). K-feldspar has an average size ranging between 8 and 12 mm. The microcline grains show patch- and braided-perthites. Quartz grains of subhedral shape; occur as clear crystals of white color. Biotite appears as subangular and elongate masses with pleochroism that is typically a light yellow color.

Fine-grained granite comprises of K-feldspar (30-35%), plagioclase (25-30%), quartz (25-30%), hornblende and biotite (8-10%), and accessory zircon, apatite, rare sphene. K-feldspar crystals are large (up to 5-6 mm across) and smaller (1-3 mm and less) subhedral microcline grains. Some large crystals of

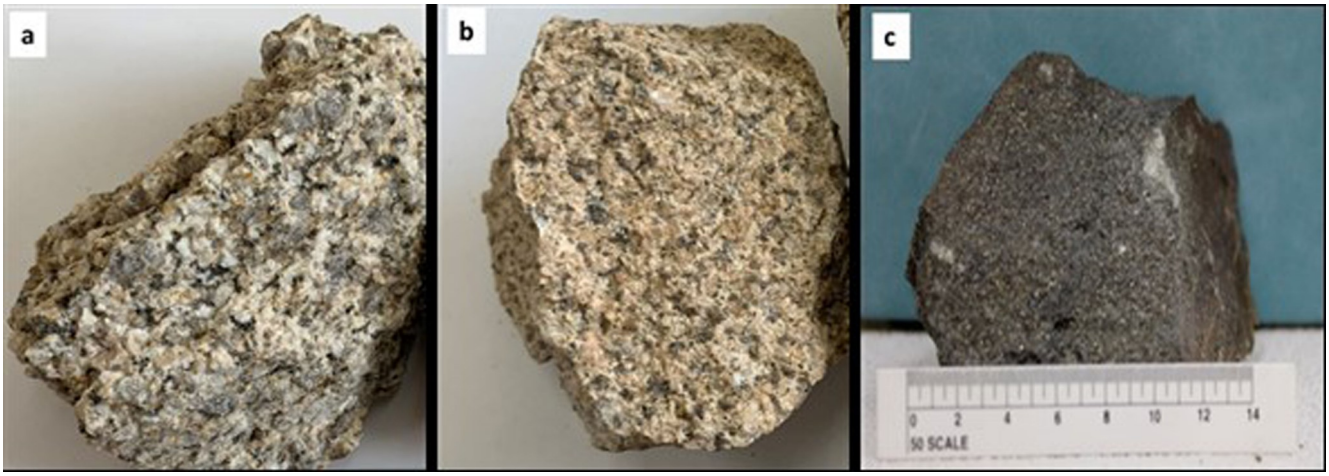

Fig. 3. Samples (a) leucogranodiorite, (b) granite, and (c) diorite of different types comprising the Telmen Complex

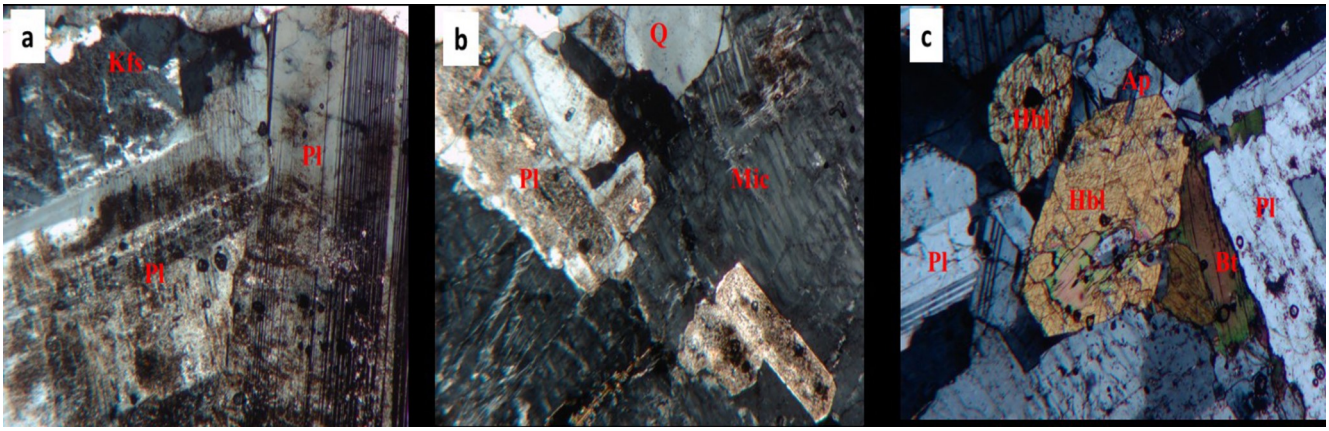

Fig. 4. Photomicrographs of samples of leucogranodiorite (a), granite (b) and diorite (c). Mineral abbreviations: Pl-plagioclase; Kfs-K-feldspar; Qz-quartz; Mic-microcline; Hbl- Hornblende; Bt-biotite; Ap-apatite

microcline exhibit characteristic grid (cross-hatched) twinning (Fig. 4b).
Plagioclase occurs in medium- and small-sized discrete grains, some crystals are untwined while others show polysynthetic twinning, and slight sericitization and saussuritization are observed. Quartz grains appear as small clear crystals with subhedral shapes. Biotite is a stretched mineral laths with light to dark-brown pleochroism and is randomly oriented with apatite, and sphene. The sphene (0.02 - 0.04 mm) is dark brown in color and elongated. Apatite (0.01-0.12 mm) is colorless, grassy, and finely prism-shaped.

Hornblende diorite /TR-20-52, 53, 54, 60, 64/. It has a medium-grained, hypidiomorphic granular texture and consists mainly of plagioclase (50–55%), hornblende (10-15%), biotite (15-20%), quartz (3-5%) (Fig. 4c). The main secondary minerals are sericite and epidote-zoisite, chlorite, and accessory zircon, apatite, and magnetite.
Plagioclase (An_{35-38}) is relatively regularly, grain size 2.5 mm prismatic crystals, lamellar twinning, the surface is mostly cleared of secondary minerals, sometimes partially covered with sericite-saussuritization. Hornblende (0.07-1.4 mm) is pale green to bluish green pleochroism, the hexagonal crystals and partially replaced by biotite.

METHODS

Major and trace elements

The SGS Laboratory in Ulaanbaatar, Mongolia carried out a whole rock analysis of the major rock and trace elements analyses for 15 samples from the Telmen Complex. Before analysis, the samples were crushed in a steel jaw crusher and then powdered in an agate mill to a grain size of 74 μm. The detailed methodologies for major element compositions are as follows: Loss of ignition (LOI) was determined after igniting the sample powders at 1000°C for 1 h. A calcined or ignited sample (0.9 g) was added to 9.0 g of Lithium Borate Flux ($Li_2B_4O_7$–$LiBO_2$), mixed well, and then fused in an auto fluxer at 1050° and 1100°C. A flat molten glass disk was prepared from the resulting melt. Then a Panalytical axios Max X-ray fluorescence instrument (XRF, Panalytical, Almelo, The Netherlands) analyzed this disk was then analyzed, with an analytical accuracy of approximately 1 to 5%. ICP-MS measured the trace element compositions (Perkin Elmer Elan 9000, Perkin, Waltham, MA, USA), with an analytical accuracy better than 5%.

LA-ICP-MS zircon U-Pb dating

Zircons were extracted from granodiorite (sample TR-19-06) using combined magnetic and heavy liquid separation techniques at the Petrography laboratory of the Institute of Geology of the Mongolian Academy of Sciences. The LA-ICP-MS zircon isotope studies were performed at the Geology Laboratory of Tianjin Center of the China Geological Survey. The zircon grains were examined under transmitted and reflected light using an optical microscope. Cathodoluminescence (CL) images were obtained using a JEOL scanning electron microscope. The zircons were selected for analysis based on their CL images. The dating results are presented in Table 2.

ANALYTICAL RESULTS

Geochemistry Characteristics

The Telmen Complex in the Tarvagatai Block comprises units of granite (granodiorite, monzogranite and granite) and diorite (monzodiorite, gabbrodiorite and diorite).

Major elements

The granitic rocks of the Telmen Complex are divided into granite and diorite units based on geochemical characteristics. The two types of rocks are classified as granite and diorite in the Q-ANOR diagram (Fig. 5a), respectively.

The Granite unit has SiO_2=71.91-76.25 wt.%, TiO_2=0.09-0.30 wt.%, Fe_2O_3=0.99-2.30 wt.%, Al_2O_3=12.93-15.00 wt.%, CaO=0.72-2.28 wt.%, Mg# [Mg#=100Mg^{2+}/(Mg^{2+}+TFe^{2+})]=9.29-20.26, Na_2O=3.01-4.45 wt.%, K_2O=2.83-4.78 wt.%, and Na_2O/K_2O=0.51-1.57. In the K_2O-SiO_2 diagram, the rocks are mainly classified as medium to high-K calc-alkaline series and ASI (aluminum saturation index) major ratios of between 1.02-1.04 (Figs. 5c and b).

The Diorite unit has SiO_2=53.06-61.90 wt.%, TiO_2=0.36-1.06 wt.%, Fe_2O_3=5.13-13.48 wt.%, Al_2O_3=10.14-19.39 wt.%, CaO=4.52-9.64 wt.%, Mg# [Mg#=100Mg^{2+}/(Mg^{2+}+TFe^{2+})]=24.47-58.5, Na_2O=1.42-4.39 wt.%, K_2O=0.65-2.51 wt.%, and Na_2O/K_2O=1.03-3.82 (Table 1). In the K_2O-SiO_2 diagram, the rocks are classified mainly as calc-alkaline series and major ratios of <0.93 (Figs. 5c and b). The two units belonged to the subalkalic series (Fig. 5d).

All rocks are enriched in Al, contains >12 wt.% Al_2O_3 and are metaluminous (Fig. 5b). The K content appears higher in granite than in diorite (K content 0.65 and 4.5 wt.% K_2O respectively). However, it decreases with increasing SiO_2 (Fig. 6). On the Harker diagrams, major elements of the Telmen Complex roughly define continuous variation trends (Fig. 6) resulting in these all granitic rocks probably came from a single magma chamber but evolved in different degrees.

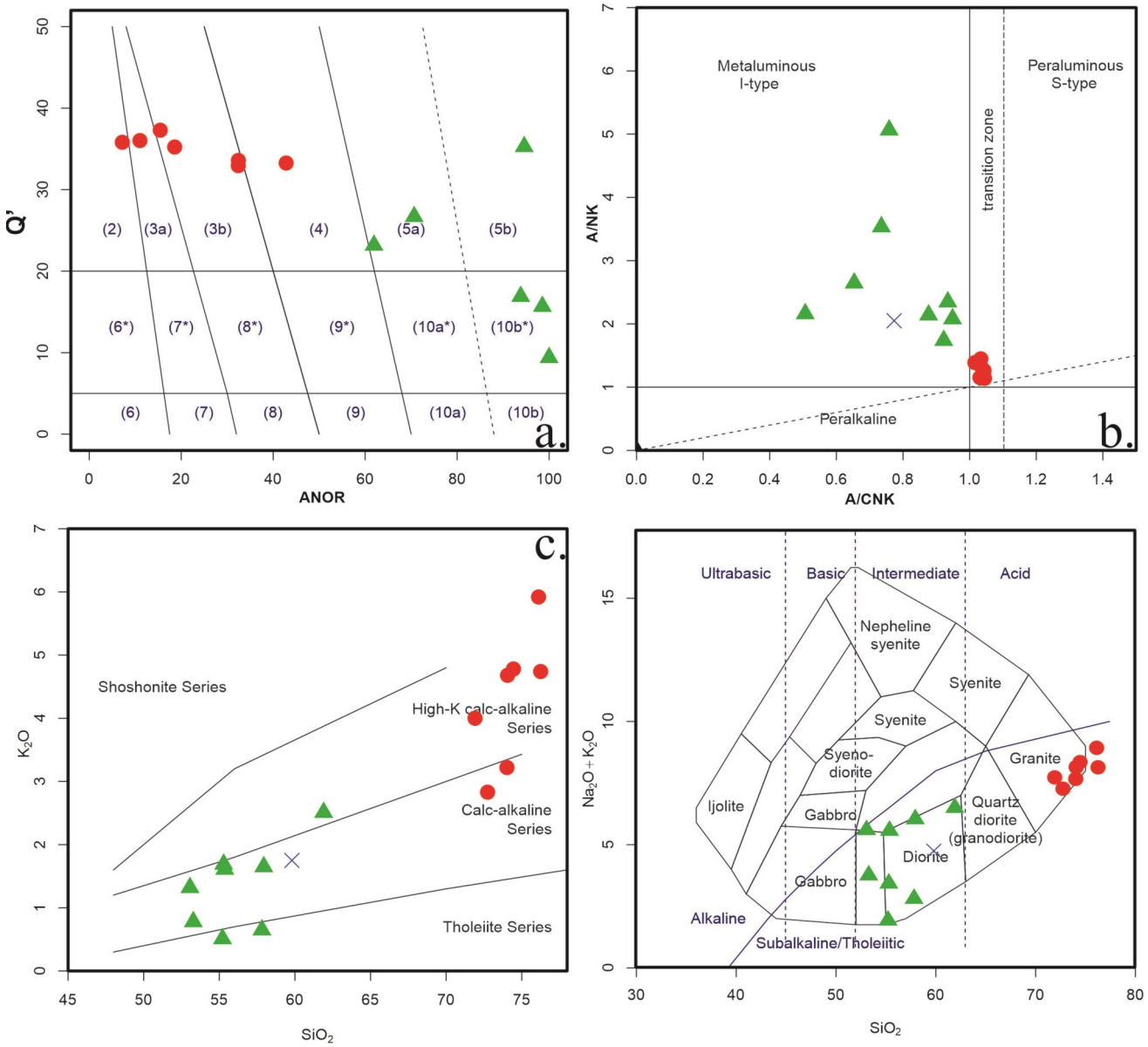

Fig. 5. Classification diagram of the Telmen Complex, a) Q'-ANOR normative composition diagram (Streckeisen and Le Maitre, 1979) for classification, where Q'=100×Q/(Q+Or+Ab+An) and ANOR=100×An/(Or+An); b) A/NK - A/CNK diagram. A/NK=Al/(Na+K) (molar ratio); c) K_2O -SiO_2 diagram. The solid line is from Peccerillo and Taylor (1976), and the dashed line is from Middlemost (1986); d) TAS diagram from (Cox et al., 1979)

REE and trace elements

The trace and REE data sets can be found in the Table 1. The Telmen Complex is characterized by enrichment in light rare earth elements (LREE), depletion in heavy rare earth elements (HREE) (Figs. 7b and d), as the LREE values from 24.00 ppm, to 185.89 ppm and the HREE values range from 1.56 ppm to 19.59 ppm. LREE/HREE values are in the range of 4.65-26.44 and REE values from 29.16 ppm to 193.55 ppm, indicating low values. The $(La/Yb)_N$ value is higher in most granite units than in diorite units (3.66-30.75) with an average of 17.40, and weak positive or normal Eu anomalies on a chondrite normalized rare earth element (REE) diagram (Figs. 7b and d). A primitive mantle-normalized trace element spider diagram indicates that these rocks are

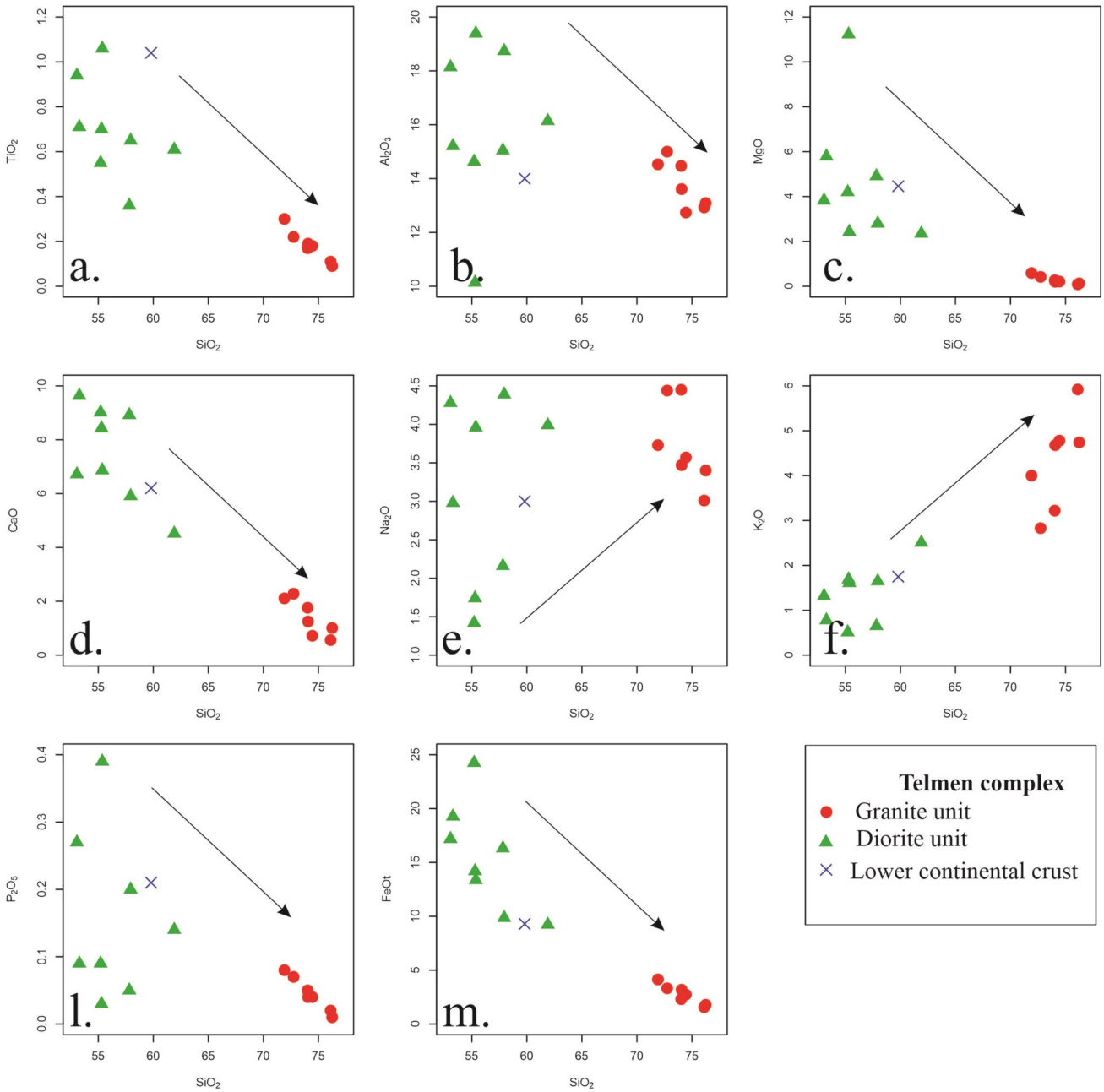

Fig. 6. Harker-type diagrams for the Telmen Complex showing the behavior of major oxides with SiO_2. The arrows represent the fractional crystallization trends of granitic rocks

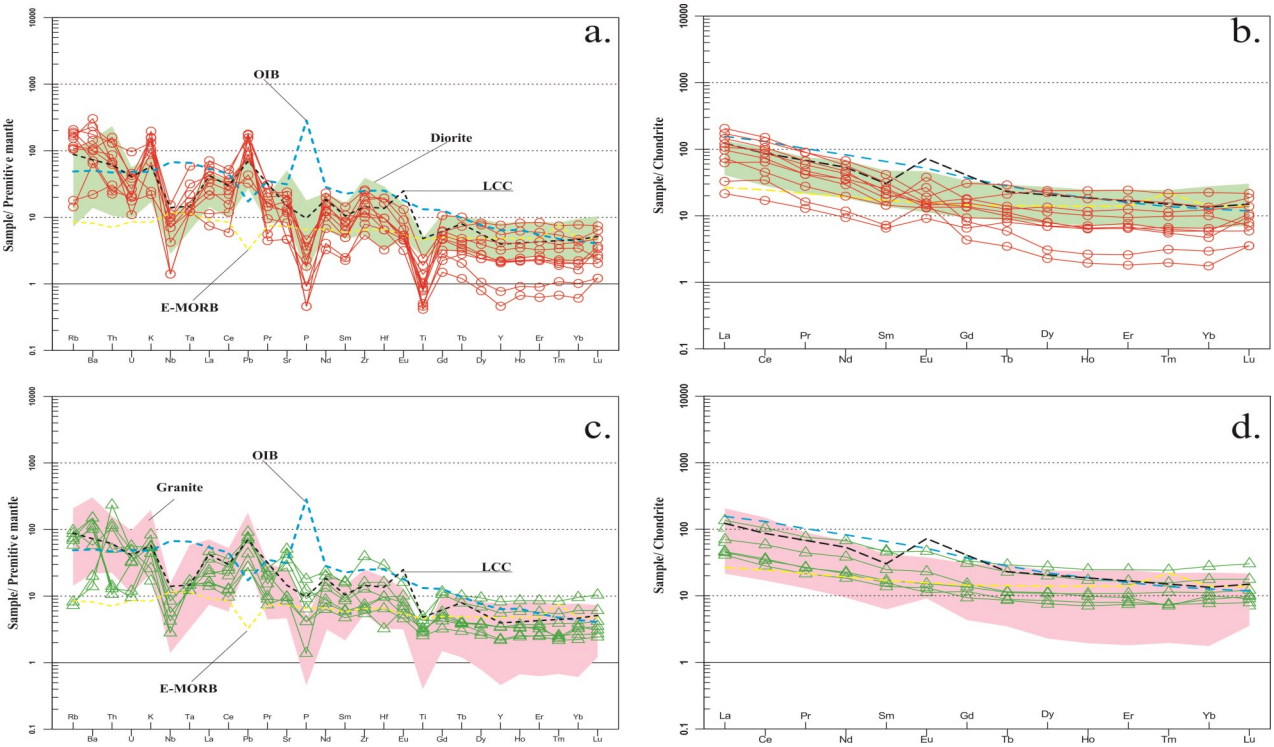

Fig. 7. REE and trace element distribution diagrams for Telmen Complex. a.c) Primitive mantle-normalized spider diagram. b. d) Chondrite-normalized REE plots of the representative samples from Telmen Complex; b) Chondrite and primitive mantle data for normalization, N-MORB, E-MORB and OIB data are all from Sun and McDonough (1989); LCC data are from Rudnick and Gao (2003)

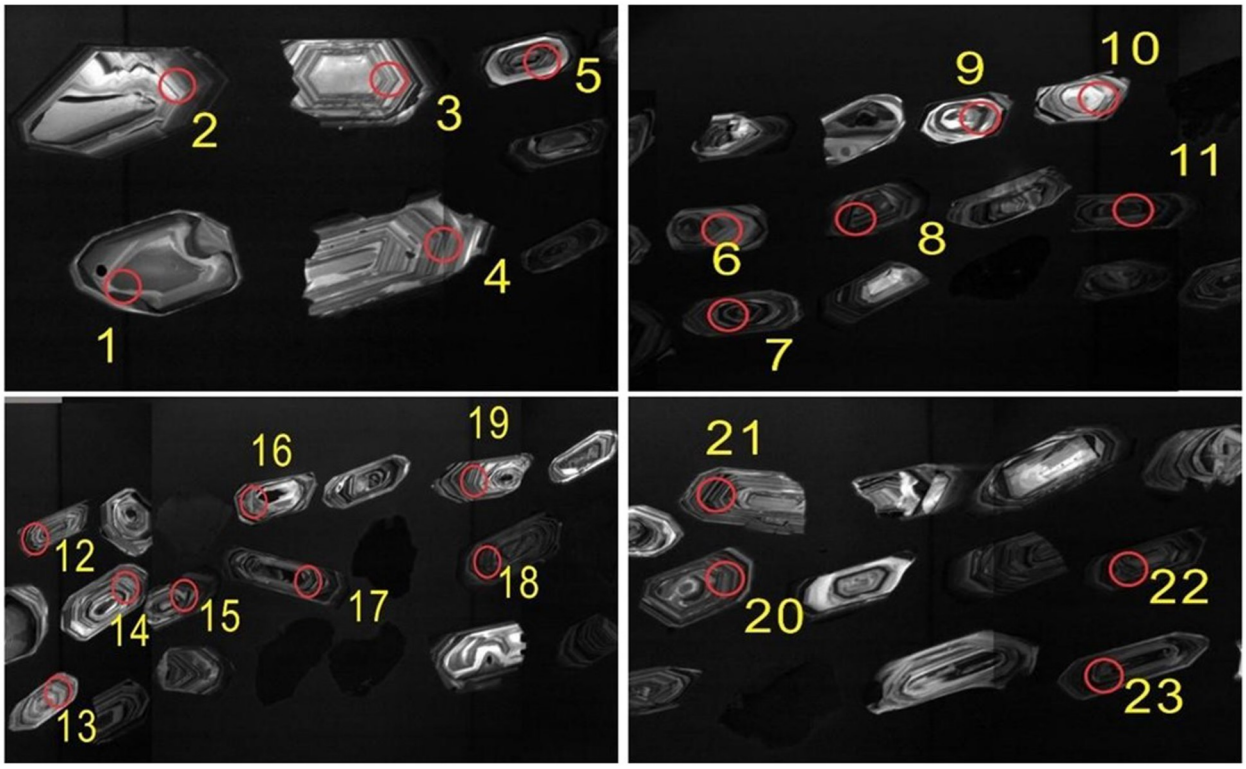

Fig. 8. Representative cathodoluminescence (CL) images of zircons from Telmen Complex granitic intrusions. Red circles show the locations of LA-ICP-MS U–Pb analyses.

enriched with Ba, K, Pb and Sr in large ion lithophile elements (LILE) and depleted with high field strength elements (HFSE) such as Nb, Ta, P, Ti, and U (Fig. 7a and c). These geochemical characteristics of the Telmen Complex are defined as typical of the lower continental crust.

Zircon U-Pb Geochronology

In this study, a granodiorite sample (TR-19-06) from the Tosontsengel massif of the Telmen Complex was chosen for the LA-ICP-MS U–Pb zircon dating. The CL images of representative zircon are shown in Fig. 8, and the U–Pb data are listed in Table 2 and plotted in Fig. 9.

Granodiorite zircons are idiomorphic and form long columnar crystals. Most zircons are 100 to 200 µm long and show fine-scale oscillatory growth zoning (Fig. 8), indicating a magmatic origin (Pupin, 1980; Corfu et al., 2003). The $^{206}Pb/^{238}U$ ages of 24 analytical points in the sample yielded ages of 430±4.9 to 419±3 Ma .A weighted mean age of 419±3 (MSWD=1.4, probability=0.12, n=17 ,error bars are 2s); Fig. 9b), which was interpreted as the crystallization age of the granodiorite.

DISCUSSION

Implication of Petrogenesis and tectonic settings

In the Telmen Complex, large-volume intrusions tend to be composite and include early quartz diorite, tonalite and granodiorite phases, as well as later granodiorite, monzodiorite and granite phases. Most units of the samples studied contain a large amount of euhedral and zoned >1 mm long plagioclase, as well as large amphiboles (Figs. 3 and 4). The granite units are plagioclase quartz-dominated rocks with biotite, and K-feldspar and diorite displays a similar mineralogy, but contains abundant amounts of amphibole and a lesser amount of quartz compared to granite units. Two units have larger plagioclase crystals that are not euhedral but are irregular in shape. Smaller crystals tend to be more euhedral. The coarse-grained size of a portion of the phases suggests crystallization at depth, and the texture indicates that the magma rose to its final emplacement depth as a crystal mush. These rock phases correspond to magmas produced under different conditions and fractional crystallization of plagioclase, later giving way to hornblende and biotite, from initial tonalitic and quartz dioritic parental materials (Fig. 6).

Hawkesworth et al., (1997) and Gill, (1981) implied that relative U and Ba/La enrichment should be realized by fluids, leading to elevated U/Th and Th/Yb ratios. The plot of U/Th vs Th and Th/Yb and Ba/La for granite and diorite units of the Telmen Complex (Figs. 10 a and b), shows that the fluids were responsible for their

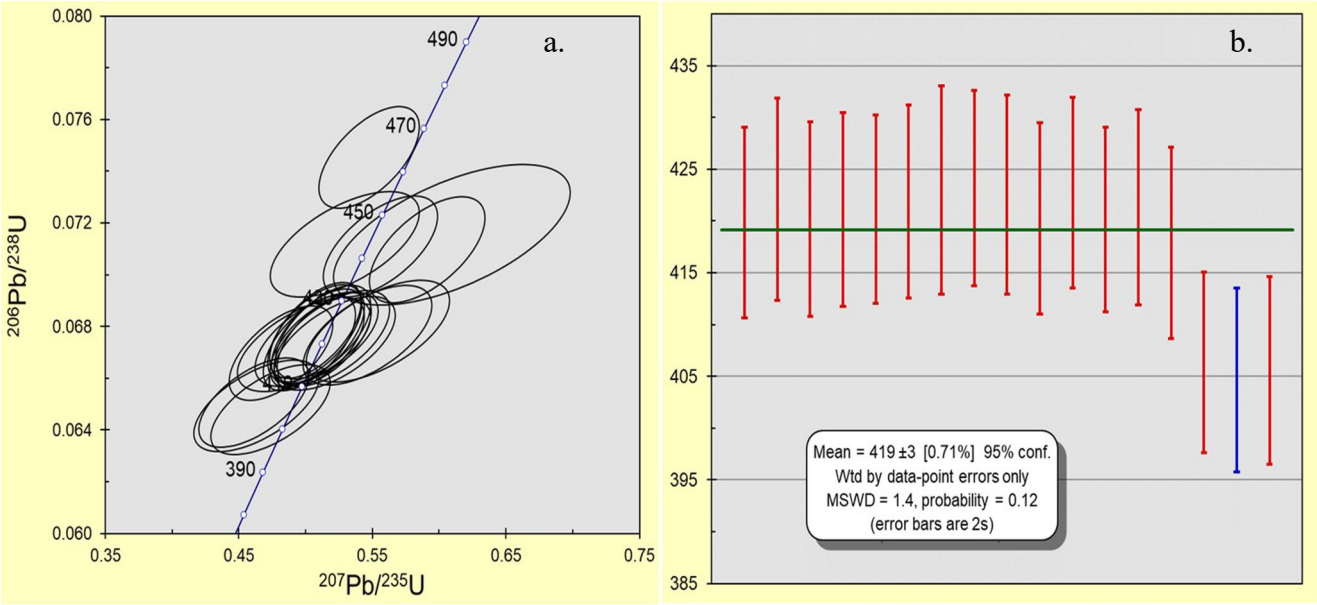

Fig. 9. Zircon LA-ICP-MS U–Pb Concordia diagrams for the samples (TR-19-06) from Telmen Complex

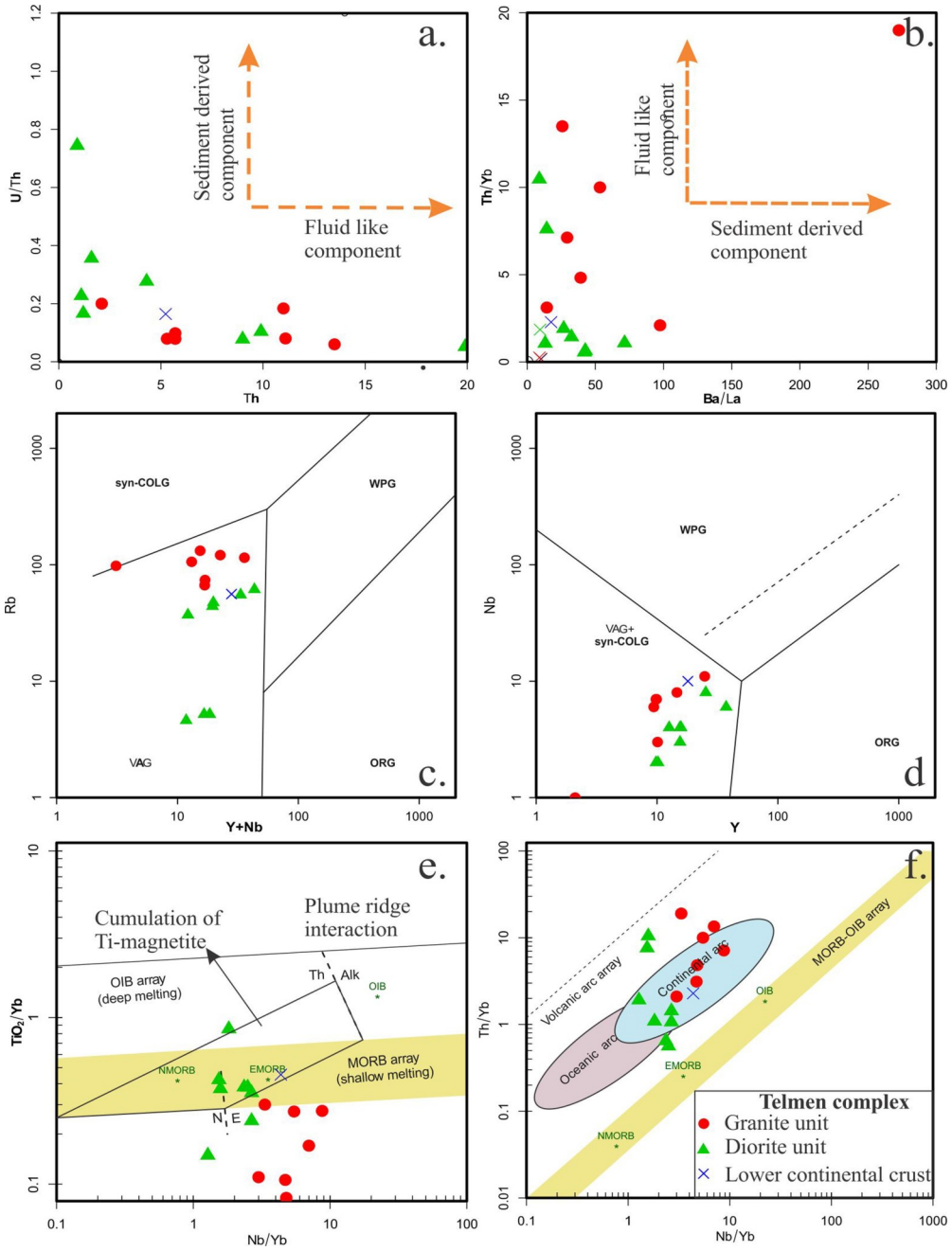

Fig. 10. a. b) U/Th versus Th and Th/Yb versus Ba/La variation diagrams of magma source, c. d) Discrimination diagram for granite (Pearce et al., 1984); ORG-ocean ridge granites; VAG-volcanic arc granites; WPG-within plate granites; syn-COLG-syn-collision granites. e. f) plots of TiO_2/Yb versus Nb/Yb and Th/Yb versus Nb/Yb after (Pearce, 2008); The mantle array extends from below normal-mid ocean ridge basalt (N-MORB) through intraplate basalts to ocean island basalts (OIB). TH: tholeiitic; CA: calc-alkaline; SHO: shoshonitic.

variations. As described above, all of the diorite and granite units of granitic rock analyzed in this study are mainly I-type granites. The most distinctive feature of island arc rocks is that they have high ratios. All of them plot within the VAG and subduction component fields on the Rb vs (Y+Nb) and Nb vs Y, TiO_2/Yb vs Nb/Yb and Th/Yb vs Nb/Yb discrimination diagrams (Figs. 10 c, d, e and f), strongly suggesting that they formed from arc related magmatism in a

subduction setting.

In previous studies, the following geochronological information was reported from the granitic rocks of the Telmen Complex in the Tarvagatai Block. It is available for the Telmen Complex where the granodiorite age is 446 Ma (Fedorov, 1966) and the zircon age of hornblende diorite is 437±7 Ma and 421±1 Ma (Kozakov et al., 2011), which may be represented by Late Ordovican to Silurian age. According to previous studies, granitic rocks in a Tarvagatai block show a crystallization age of 446-421 Ma from the Telmen complex.

Our results of the weighted average age of 419±3 Ma for granodiorite (Fig. 9), which is slightly younger than the previous age. Zircon grains with a high Th/U ratio (>0.10) are normally considered igneous origin, while metamorphic zircon grains are in many cases characterized by their low Th/U ratio (<0.10) (e.g., Hoskin and Schaltegger, 2003). Applying this measured chemical constraint, the rocks show a high Th/U ratio (>0.54), which supports the age fact that the obtained indicates the age of igneous crystallization.

CONCLUSION

On the basis of the petro-geochemical data and zircon U-Pb ages presented in this study, we draw the following conclusions.

1. The Telmen Complex of the Tarvagatai Block consists of commonly two granitic units of granite-granodiorite and gabbro-dioite units, which intruded into a basement rock composed of granite and diorite gneiss.
2. The two units belonged to the subalkalic series and aluminum-supersaturated with a high degree of evolution, whose geochemical characteristics suggest that it is an I-type granite. Granite units are highly K calc-alkaline and weakly metaluminous, with A/CNK ratios ranging from 1.02 to 1.04. The diorite units are classified as calc-alkaline series and ASI major ratios of <0.93. The Telmen Complex roughly defines continuous variation trends, resulting in granitic rocks probably came from a single magma chamber but evolved to different degrees.
3. In the granitic rocks, the calc-alkaline geochemical signature and characteristic enrichment in LILE (including, K, Sr, and Pb) and U with Th relative to the HFSE (Nb and Ta) indicate an origin within an igneous arc. These geochemical characteristics of the Telmen Complex are defined as typical of the lower continental crust.
4. LA-ICP-MS zircon U-Pb dating revealed a new age in which medium-grained granodiorite from the Telmen Complex (419±3, MSWD=1.4, probability=0.12, n=17 Ma) formed in the Late Silurian.
5. Regional geologically, according to previous and our studies inferred that the granitic complexes correspond formed in an arc collision/transitional setting from syn-collision to post-collision during the Cambrian - Silurian.

ACKNOWLEDGEMENTS

We thank the handling editor and referees for their constructive comments and suggestions which improved this paper. This study was financially sponsored by The Mongolian Foundation for Science and Technology and Ministry of Education and Science of Mongolia (Research project No.2019/02). We thank Li Junjian for helping with LA-ICP- MS zircon dating.

REFERENCES

Anisimova, I.V., Kozakov, I.K., Yarmolyuk, V.V., Kozlovsky, A.M., Kovach, V.P., Kudryashova, E.A., Savatenkov, V.M., Terent'eva, L.B., Fedoseenko, A.M., Yakovleva, S.Z., Enzhin, G. 2009. Age, sources, and geological position of anorthosites of Precambrian terranes of Central Asia: Example from the Khunzhilingol Massif, Mongolia. Dokady Earth Sciences, v. 428 (1), p. 1120-1125. https://doi.org/10.1134/S1028334X09070186

Buriánek, D., Krejčí, Z., Jiang, Y., Otgonbaatar, D. 2020. Geology of the Gobi and Mongol Altai junction enhanced by gravity analysis: a key for understanding of the Mongolian Altaides. Journal of Maps, v. 16(2), p. 98–107. https://doi.org/10.1080/17445647.2019.1700835

Chen, N.H.C., Zhao, G., Jahn B.M., Zhou, H., Sun, M. 2017. Geochemistry and

geochronology of the Delinggou Intrusion: Implications for the subduction of the Paleo-Asian Ocean beneath the North China Craton. Gondwana Research, v. 43, p. 178-192. https://doi.org/10.1016/j.gr.2016.01.007

Corfu, F., Hanchar, J.M., Hoskin, P.W.O., Kinny, P. 2003. Atlas of zircon textures. Reviews in Mineralogy and Geochemistry, v. 53, p. 469-500. https://doi.org/10.2113/0530469

Cox, K.G., Bell, J.D., Pankhurst, R.J. 1979. The interpretation of data for plutonic rocks. In The Interpretation of Igneous Rocks. Springer, p. 308-331. https://doi.org/10.1007/978-94-017-3373-1_13

Erdenechimeg, D., Boldbaatar, G., Enkhbayar, B., Damdinjav, B., Taivanbaatar, Ts., Oyungerel, N. 2017. Geology map of Mongolia, scale 1:500 000. Eds. Tumurtogoo,O., Orolmaa, D. Geoinformation database-2013 project. Geological Information Center, Mongolia.

Fedorov, E. 1966. Geological formations of the western part of the Tarvagatai mountain range, Khungui and Galuut river delta (M-46 -G, M-47-B, L-47-A planes) 1: 1,000,000 scale geological mapping report performed in 1966 under Contract No. 91497 dated April 23, 1966).

Gill, J.B. 1981. What is "Typical Calcalkaline Andesite"? In Orogenic Andesites and Plate Tectonics, Springer p. 1-12. https://doi.org/10.1007/978-3-642-68012-0_1

Guan, Q.B., Liu, Z.H., Wang, X.A., Wang, B., Wang, S.J. 2018. Zircon U-P-Hf isotopic and geochemical characteristics of the Xierzi biotite monzogranite pluton, Linxi, Inner Mongolia and its tectonic implications. Geoscience Frontiers, v. 9, p. 505-516. https://doi.org/10.1016/j.gsf.2017.05.004

Hanžl, P., Guy, A., Battushig, A., Lexa, O., Schulmann, K., Kunceová, E., Hrdličková, K., Janoušek, V., Hawkesworth, C.J., Turner, S.P., McDermott, F., Peate, D.W., Van Calsteren, P. 1997. U-Th isotopes in arc magmas: Implications for element transfer from the subducted crust. Science, v. 276 (5312), p. 551-555. https://doi.org/10.1126/science.276.5312.551 PMid:9110968

Hoskin, P.W O., Schaltegger, U. 2003. The composition of zircon and igneous and metamorphic petrogenesis. Reviews in Mineralogy and Geochemistry, v. 53, p. 27-55. https://doi.org/10.2113/0530027

Jahn, B.M., Capdevila, R., Liu, D., Vernon, A., Badarch, G. 2004. Sources of Phanerozoic granitics in the transect Bayanhongor-Ulaanbaatar, Mongolia: Geochemical and Nd isotopic evidence and implications for Phanerozoic crustal growth. Journal of Asian Earth Sciences, v. 23(5), p. 629–653. https://doi.org/10.1016/S1367-9120(03)00125-1

Jahn, B.M., Wu, F., Chen, B., 2000a. Granitoids of the Central Asian Orogenic Belt and continental growth in the Phanerozoic. Transactions of the Royal Society of Edinburgh: Earth Sciences, v. 91(1-2), p. 181 –193. https://doi.org/10.1017/S0263593300007367

Jahn, B.M., Wu, F., Chen, B., 2000b. Massive granitoid generation in Central Asia: Nd isotope evidence and implication for continental growth in the Phanerozoic. Episodes, v.23(2), p. 82-92. https://doi.org/10.18814/epiiugs/2000/v23i2/001 PMid:25688382

Kheraskov, N.N. 1966. Geological sheet map, 1:1000,000. Open file report in geological finds of Mongolia no.1752. (in Russian)

Kozakov, I.K., Kozlovsky, A.M., Yarmolyuk, V.V. 2011. Crystalline complexes of the Tarbagatai Block of the Early Caledonian superterrane of Central Asia. Petrology, v. 19 (4), p. 426-443. https://doi.org/10.1134/S0869591111040047

Kröner, A., Kovach, V., Belousova, E., Hegner, E., Armstrong, R., Dolgopolova, A., Seltmann, R., Alexeiev, D.V., Hoffmann, J.E., Wong, J., Sun, M., Cai, K., Wang, T., Tong, Y., Wilde, S.A., Degtyarev, K.E., Rytsk, E. 2014. Reassessment of continental growth during the accretionary history of the Central Asian Orogenic Belt. Gondwana Research, v. 25, p. 103-125. https://doi.org/10.1016/j.gr.2012.12.023

Liu, Y.J., Li, W.M., Feng, Z.Q., Wen, Q.B., Neubauer, F., Liang, C.Y. 2016. A Review of the Paleozoic Tectonics in the Eastern Part of Central Asian Orogenic Belt. Gondwana Research, v. 43, p. 123-148. https://doi.org/10.1016/j.gr.2016.03.013

Middlemost, E.A.K. 1986. Magmas and Magmatic Rocks: An Introduction to Igneous Petrology. Longman Group Ltd., London, New York, p. 266.

Pearce, J.A, Harris, N.B.W., Tindle, A.G. 1984. Trace element distribution diagrams for the tectonic interpretation of granitic rocks. Journal of Petrology, v. 25(4), p. 956-983. https://doi.org/10.1093/petrology/25.4.956

Pearce, J.A. 2008. Geochemical fingerprinting of oceanic basalts with applications to ophiolite classification and the search for Archean oceanic crust. Lithos, v. 100(1-4), p. 14-48. https://doi.org/10.1016/j.lithos.2007.06.016

Peccerillo, A., Taylor, S.R. 1976. Geochemistry of Eocene calc-alkaline volcanic rocks from the Kastamonu area, northern Turkey. Contributions to Mineralogy and Petrology, v. 58(1), p. 63-81. https://doi.org/10.1007/BF00384745

Pupin, J.P. 1980. Zircon and Granite Petrology. Contribution to Mineralogy and Petrology, v.73, p. 207-220. https://doi.org/10.1007/BF00381441

Rudnick, R.L., Gao, S. 2003. Composition of the Continental Crust. In Treatise on Geochemistry 3. 2nd Ed., v. 3, p. 1-64. https://doi.org/10.1016/B0-08-043751-6/03016-4

Schulmann, K., Paterson, S. 2011. Asian Continental Growth. Nature, v. 4(12), p. 827 –829. https://doi.org/10.1038/ngeo1339

Şengör, A.M.C., Natal´in, B,A., Burtman, V.S. 1993. Evolution of the Altaid tectonic collage and Paleozoic crustal growth in Eurasia. Nature, v. 364, p. 299-307. https://doi.org/10.1038/364299a0

Streckeisen, A., Le Maitre, R.W. 1979. A chemical approximation to the modal QAPF classification of the igneous rocks. Neues Jahrbuch fur Mineralogie, Abhandlungen, v.136, p. 169-206.

Sun, S.S., McDonough, W.F. 1989. Chemical and isotopic systematics of oceanic basalts: Implications for mantle composition and processes. Geological Society Special Publication, v. 42(1), p. 313–345. https://doi.org/10.1144/GSL.SP.1989.042.01.19

Sun, D.Y., Wu, F.Y., Zhang, Y.B., Gao, S. 2004. The final closing time of the west Lamulun River-Changchun-Yanji plate suture zone: Evidence from the Dayushan granitic pluton, Jilin Province. Journal of Jilin University (Earth Science Edition), v,. 34, p. 174-181.

Windley, B.F., Alexeiev, D., Xiao, W.J., Kröner, A., Badarch, G. 2007. Tectonic models for accretion of the Central Asian Orogenic Belt. Journal of Geological Society. v. 164, p. 31-47. https://doi.org/10.1144/0016-76492006-022

Yarmolyuk V.V., Kozlovsky A.M., Travin A.V., Kirnozova, T.I., Fugzan, M.M., Kozakov, I.K., Plotkina, Yu.V., Eenjin, G., Oyunchimeg, Ts., Sviridova, O.E. 2019. Duration and geodynamic nature of giant Central Asian Batholiths: Geological and geochronological studies of the Khangai Batholith. Stratigraphy and Geological Correlation, v. 27(1), p. 73-94. https://doi.org/10.1134/S0869593819010088

Yarmolyuk, V.V., Kuzmin, M.I., Kozlovsky, A.M. 2013. Late Paleozoic-Early Mesozoic within-plate magmatism in north Asia: traps, rifts, giant batholiths, and the geodynamics of their origin, Petrology, v. 21(2), p. 101-126. https://doi.org/10.1134/S0869591113010062

Yarmolyuk, V.V., Kozakov, I.K., Kozlovsky, A.M. 2018. The Early Paleozoic Active Margin of the Khangai Segment of the Mongol-Okhotsk Ocean. Doklady Earth Science. v. 480, p. 559–563. https://doi.org/10.1134/S1028334X18050094

Yarmolyuk, V.V., Kozlovsky, A.M., Savatenkov, V.M., Kovach, V.P., Kozakov, I.K., Kotov, A.B., Lebedev, V.I., Eenjin, G. 2016. Composition, Sources, and Geodynamic Nature of Giant Batholiths in Central Asia: Evidence from the Geochemistry and Nd Isotopic Characteristics of Granitics in the Khangai Zonal Magmatic Area .Petrology. v. 24(5), p. 468-498. https://doi.org/10.1134/S0869591116050064